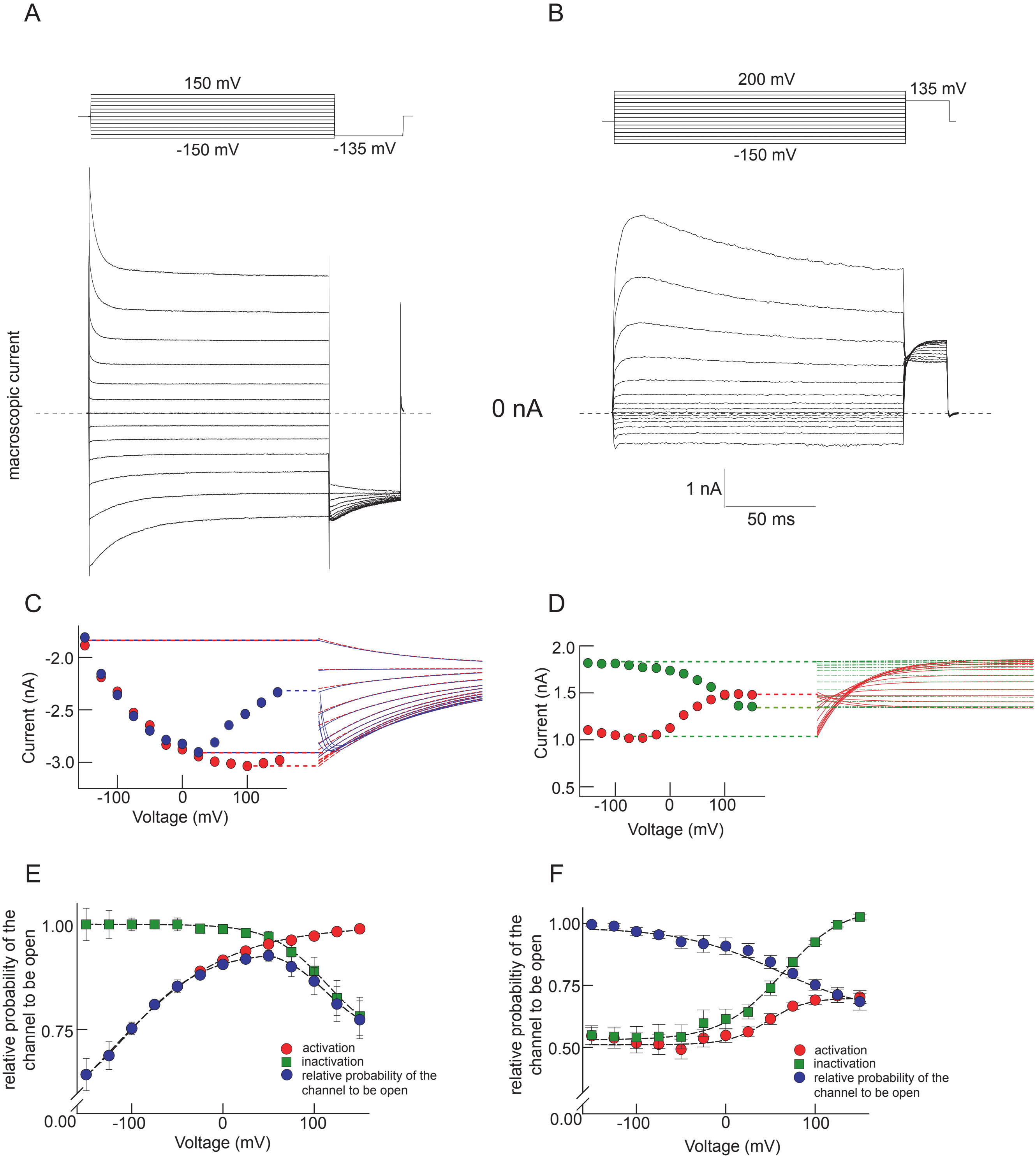

Supplementary Fig. S1: Kovermann et al

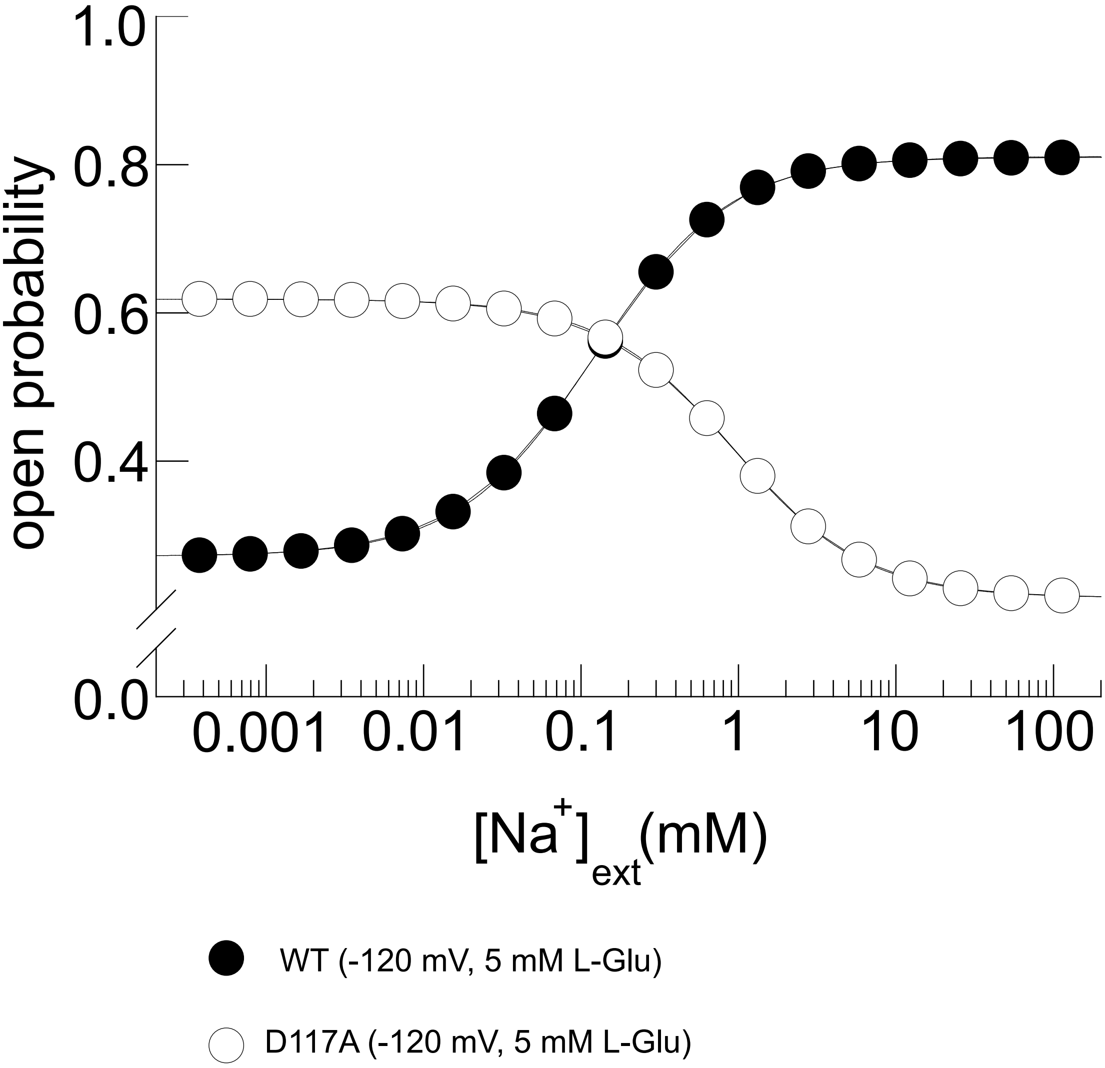

Supplementary Fig. S2: Kovermann et al

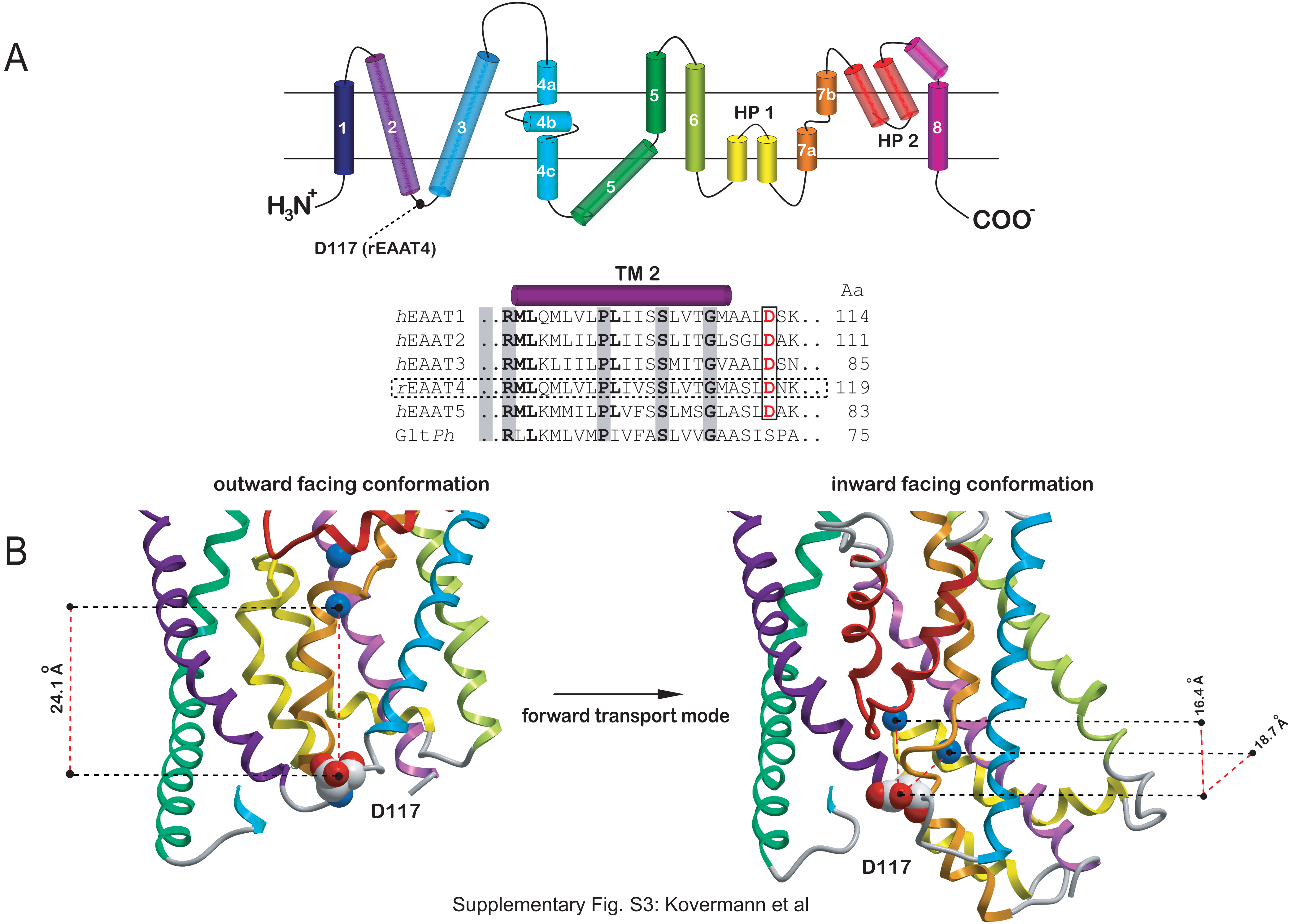

Supplementary Fig. S3: Kovermann et al

A

Table S1A: rate constants for model 1 and 2 (Fig. 7A-D)

	forward	*backward*	zδ	*asymmetry*
1	$1.0 \times 10^{4}\ M^{-1}s^{-1}$	$1.0 \times 10^{2}\ s^{-1}$	0.46	0.1
2	$1.0 \times 10^{4}\ M^{-1}s^{-1}$	$5.0 \times 10^{2}\ s^{-1}$		
3	$6.0 \times 10^{6}\ M^{-1}s^{-1}$	$5.0 \times 10^{2}\ s^{-1}$		
4	$6.0 \times 10^{11}\ M^{-1}s^{-1}$	$7.0 \times 10^{2}\ s^{-1}$		
5	$6.0 \times 10^{11}\ M^{-1}s^{-1}$	$7.0 \times 10^{2}\ s^{-1}$		
6	$6.0 \times 10^{6}\ M^{-1}s^{-1}$	$5.0 \times 10^{2}\ s^{-1}$		
7	$1.0 \times 10^{4}\ M^{-1}s^{-1}$	$1.0 \times 10^{3}\ s^{-1}$	0.55	0.5
8	$2.0 \times 10^{3}\ M^{-1}s^{-1}$	$1.9 \times 10^{3}\ s^{-1}$		
9	$1.0 \times 10^{3}\ s^{-1}$	$4.0 \times 10^{4}\ M^{-1}s^{-1}$	0.40	0.5
10	$3.0 \times 10^{3}\ s^{-1}$	$9.0 \times 10^{10}\ M^{-1}s^{-1}$		
11	$3.0 \times 10^{3}\ s^{-1}$	$1.0 \times 10^{5}\ M^{-1}s^{-1}$		
12	$1.0 \times 10^{5}\ s^{-1}$	$2.0 \times 10^{7}\ M^{-1}s^{-1}$		
13	$1.0 \times 10^{5}\ s^{-1}$	$1.0 \times 10^{8}\ M^{-1}s^{-1}$		
14	$1.0 \times 10^{6}\ M^{-1}s^{-1}$	$1.0 \times 10^{3}\ s^{-1}$		
15	$4.0 \times 10^{1}\ s^{-1}$	$1.0 \times 10^{1}\ s^{-1}$	0.59	0.9
16	$2.0 \times 10^{4}\ s^{-1}$	$1.0 \times 10^{6}\ M^{-1}s^{-1}$		
17	$1.4 \times 10^{1}\ s^{-1}$	$1.0 \times 10^{-2}\ s^{-1}$	0.05	0.5

B

Table S1B: open probabilities for model 1 and 2 (Fig. 7A-D)

	model 1		*model 2*	
	WT	*D117A*	*WT*	*D117A*
p1	0.65	0.005	0.55	0.03
p2	0.24	0.77	0.80	0.79
p3	0.96	1.00	0.16	0.22
p4	0.05	0.49	0.26	0.30
p5	0.15	0.75	0.13	0.66
p6	1.00	0.01	1.00	0.002
p7	0.19	0.23	0.66	0.23
p8	*n. d.*	*n. d.*	*n. d.*	*n. d.*

Supplementary Table S1: Kovermann et al

FIGURE S1. **Separation of two gating processes with distinct voltage dependence in WT and mutant D117A EAAT4 anion channels.** *A, B,* gate separation in WT (*A*) and D117A EAAT4 (*B*). Tail currents at -135 mV (WT) or +135 mV (D117A) were fit with mono- or biexponential function to determine instantaneous (WT) or late (D117A) current amplitudes. *C*, *D*, plot of instantaneous and late current amplitudes for WT (*C*) and D117A (*D*) EAAT4. *E*, *F*, voltage dependence of relative open probabilities as well as of channel activation and inactivation for WT (*E*) and D117A (*F*) EAAT4.

FIGURE S2. **Modified channel open probabilities in D117A explain the experimentally observed alterations of Na^+ dependences.** Simulated sodium dependences for WT and D117A EAAT4 anion currents at -120 mV using model 2 shown in Fig. 7C.

FIGURE S3. **Distances between D117A and Na^+-binding sites estimated from homology modeling of EAAT4.** *A,* position of D117 in the predicted topology model of EAAT4 based on (9) and alignment of amino acid sequences homologous to AA 95 and 119 in *r*EAAT4. *B,* tertiary structure of *r*EAAT4 as homology modeled to Glt_{Ph} high resolution structures with PDB IDs 2NWX (outward facing conformation) and 3KBC (inward facing conformation). Colors of TMs are according to A, TM1 and TM4 were removed for clarity. Interhelical loops are in grey. D117 and bound Na^+ are depicted as space-filling models.

TABLE S1. **Rate constants and open probabilities used in the kinetic modeling of WT EAAT4 and D117A EAAT4.** *A*, rate constants and fit parameter for $z\delta$ and for asymmetries applied to model 1 and 2. Electrogenic reactions are defined by $z\delta$ values, which give the effective charge movement across the membrane and asymmetry values referring to the different voltage dependence of the forward and the backward reaction. *B*, Simulated open probabilities for model 1 and 2.